Protein nanoparticles engineered to sense kinase activity in MRI

Mikhail G. Shapiro, Jerzy O. Szablowski, Robert Langer, Alan Jasanoff*

SUPPORTING INFORMATION

EXPERIMENTAL METHODS

Fusion gene construction

Light-chain Ft fusion constructs were generated using standard molecular cloning techniques. Original genes encoding human Ft were kindly supplied by Paulo Arosio; genes encoding rat CREB and mouse CBP were obtained from Michael Greenberg. KID-LF encodes amino acids 88-160 of CREB, followed by the spacer GTSSEFM, and LF. KIX-LF encodes amino acids 574-686 of CBP, followed by the same spacer and LF. FLAG-LF encodes the amino acid sequence MDYKDHDGDYKDHDIDYKDDDDK (3xFLAG, Sigma-Aldrich, St. Louis, MO) in place of KID or KIX. All three LF fusion constructs, along with unmodified LF and HF, were cloned into the pCMV-Sport vector (Invitrogen, Carlsbad, CA) for expression in mammalian cells under the human cytomegalovirus promoter.

Ft nanoparticle expression and purification

Ft nanoparticles were expressed in suspension-cultured HEK-293 cells using the FreeStyle 293 system (Invitrogen), in accordance with manufacturer instructions. Plasmids encoding HF, LF, FLAG-LF and either KID-LF or KIX-LF were mixed and transfected into cells at predetermined ratios (by DNA mass), in a method used commonly for expression of other multi-subunit proteins in mammalian cells (*e.g.* ion

channels). For a 60% functional group composition, the plasmid mixture contained 60% KID-LF or KIX-LF, 20% FLAG-LF, 10% HF and 10% LF. Lower functional group compositions were compensated by unmodified LF. Assuming quadrinomial statistics (four possible constructs at each monomer position in Ft), and that incorporation of Ft constructs is proportional to the transfected dose of the corresponding plasmid, a minimum of 84% of expressed FtN particles was expected to contain one or more of each of the four relevant constructs. Four days after transfection, cells were harvested and lysed in lysis buffer (50 mM Tris-HCl, 150 mM NaCl, 1 mM EDTA, 1% Triton X-100, pH 7.4; 6 mL per pellet generated from a 50 mL culture) supplemented with a protease inhibitor cocktail (Halt, Pierce, Rockford, IL). Cleared lysates were supplemented overnight with 2 mM ferrous ammonium sulfate (Sigma-Aldrich) at 4 °C. Anti-FLAG agarose (EZview, Sigma-Aldrich) was added for an additional 2 hours. After washing with wash buffer (50 mM Tris-HCl, 150 mM NaCl, pH 7.4), the nanoparticles were eluted with 0.1 M glycine at pH 3.5, then quenched with 10X wash buffer. Prior to subsequent handling, nanoparticles were concentrated using centrifugal filter units and buffer was exchanged to the assay buffer (10 mM HEPES, 150 mM NaCl, pH 7.4) using size-exclusion chromatography. Particle concentration was estimated by absorbance at 280 nm, as calibrated by an enzyme-linked immunosorbant assay (ELISA) for Ft (Leinco, St. Louis, MO). Protein expression level was quantified by comparing ELISA results to a measurement of total cellular protein in cell lysates, obtained using the bicinchoninic acid assay (Pierce, Rockford, IL). FtN concentrations are given on a per-nanoparticle basis.

Transmission electron microscopy and measurement of iron content

Samples were sonicated for five minutes in a water-bath sonicator (Cole-Parmer, Vernon Hills, IL). 5 µl of the sonicated sample was adsorbed to a formvar/carbon coated grid (Ernest F. Fullam, Latham, NY) for one minute. Excess liquid was removed from the grid with Whatman #1 filter paper. Grids were examined using a Tecnai G^2 Spirit BioTWIN transmission electron microscope (FEI, Hillsboro, OR). Nanoparticle iron content was estimated using a ferrozine-based spectroscopic assay. Protein shells were denatured in sulfuric acid and free iron reduced using thiglycolic acid. Excess ferrozine was added, and iron concentration was estimated using an extinction coefficient of 2.79 x 10^4 $M^{-1}cm^{-1}$.

Phosphorylation and dephosphorylation

Phosphorylation was carried out by the addition of the recombinant catalytic subunit of protein kinase A (PKA, Promega, Madison, WI) and 1 mM ATP (EMD Chemicals, San Diego, CA). For pre-phosphorylation, ~50 units of PKA were used per pmol of Ft. In DLS and MRI experiments, PKA was added directly from its original stock solution. To inhibit PKA activity, we used a peptide PKA inhibitor (Promega). Dephosphorylation was accomplished using lambda protein phosphatase (λPPase, New England Biolabs, Ipswich, MA), which was diluted in assay buffer and concentrated ~10-fold relative to its stock solution. Protein phosphorylation states were assayed by electrophoresis on 15% SDS-PAGE gels (BioRad, Hercules, CA) and staining using the Pro-Q Diamond phosphoprotein staining kit (Invitrogen). In gel images shown here,

lanes have been rearranged digitally to align them in the order of data presented in accompanying figures.

Dynamic light scattering

DLS measurements were performed using a DynaPro DLS system (Wyatt Technology, Santa Barbara, CA) at 25 °C. For each sample (20 μL), a single intensity-weighted value was used to characterize the relative size of clusters in the specimen. This value was an average of 60 measurements acquired over one minute.

Magnetic resonance imaging

Samples (45 μL) were arrayed into microtiter plates and placed in a 40 cm bore Bruker (Billerica, MA) Avance 4.7 T MRI scanner, equipped with a 10 cm inner diameter birdcage resonator radiofrequency coil and 26 G/cm triple axis gradients. Unused wells of the microtiter plates were filled with phosphate buffered saline, and imaging was performed on a 1.63 mm slice through the sample. A T_2-weighted spin echo pulse sequence with multiecho acquisition was used; repetition time (*TR*) was 4 s, and *TE* ranged from 30 to 900 ms, in 30 ms increments. Each acquisition lasted 8.5 minutes. Data matrices of 512 x 128 points were acquired and zero-filled to 2048 x 1024 points, where the second dimension corresponds to the phase encoding direction. Images were reconstructed and analyzed using custom routines running in Matlab. Relaxivities reported here were calculated by exponential fitting to the image data, and are given on a per-nanoparticle basis. Contrast was linearly adjusted to produce MRI images presented in the figures.

AMINO ACID SEQUENCES OF FT FUSION CONSTRUCTS

Functional domains are highlighted in blue, linkers are highlighted in orange, and LF is in black.

KID-LF:

MGSSCKDLKRLFSGTQISTIAESEDSQESVDSVTDSQKRREILSRRPSYR 50

KILNDLSSDAPGVPRIEEEKSEEETGTSSEFMSSQIRQNYSTDVEAAVNS 100

LVNLYLQASYTYLSLGFYFDRDDVALEGVSHFFRELAEEKREGYERLLKM 150

QNQRGGRALFQDIKKPAEDEWGKTPDAMKAAMALEKKLNQALLDLHALGS 200

ARTDPHLCDFLETHFLDEEVKLIKKMGDHLTNLHRLGGPEAGLGEYLFER 250

LTLKHD

KIX-LF:

MSTIPTAAPPSSTGVRKGWHEHVTQDLRSHLVHKLVQAIFPTPDPAALKD 50

RRMENLVAYAKKVEGDMYESANSRDEYYHLLAEKIYKIQKELEEKRRSRL 100

HKQGILGNQPALPAGTSSEFMSSQIRQNYSTDVEAAVNSLVNLYLQASYT 150

YLSLGFYFDRDDVALEGVSHFFRELAEEKREGYERLLKMQNQRGGRALFQ 200

DIKKPAEDEWGKTPDAMKAAMALEKKLNQALLDLHALGSARTDPHLCDFL 250

ETHFLDEEVKLIKKMGDHLTNLHRLGGPEAGLGEYLFERLTLKHD

FLAG-LF:

MDYKDHDGDYKDHDIDYKDDDDKGTSSEFMSSQIRQNYSTDVEAAVNSLV 50

NLYLQASYTYLSLGFYFDRDDVALEGVSHFFRELAEEKREGYERLLKMQN 100

QRGGRALFQDIKKPAEDEWGKTPDAMKAAMALEKKLNQALLDLHALGSAR 150

TDPHLCDFLETHFLDEEVKLIKKMGDHLTNLHRLGGPEAGLGEYLFERLT 200

LKHD

SUPPORTING RESULTS: IMPACT OF THE CHOICE OF PURIFICATION MOIETY ON STABILITY OF SELF-ASSEMBLED FTNS

Ferritin nanoparticles (FtNs) described in the main text were self-assembled from co-transfected fusions of LF with KID, KIX, and FLAG, where the FLAG-LF construct provided a means for purification of intact multifuntional FtNs. We also tested hexahistidine (6His) as a potential purification moiety. A 6His-LF fusion construct was generated with a GTSSEF linker and co-transfected into HEK293 cells together with wild-type and functional subunits as described for FLAG-LF. Self-assembled FtNs were then purified over a Ni-NTA resin (Qiagen). From cells transfected with plasmid mixtures containing 60% KID-LF DNA, KID-functionalized FtNs were obtained as expected. Cells transfected with mixtures containing 60% KIX-LF DNA yielded FtNs displaying few or no KIX groups, however (Supplementary Figure 1). When transfection mixtures contained FLAG-LF instead of 6His-LF, both KID-FtNs and KIX-FtNs expressed and behaved as expected, as described in the main text. The favorable behavior of KIX-FtN constructs containing FLAG-LF *vs.* 6His-LF may have been due to the greater negative charge, hydrophilicy, or bulkiness of FLAG compared with 6His. These results highlight the engineering value of being able to easily substitute functionalites in self-assembled FtNs.

SUPPLEMENTARY FIGURE CAPTIONS

Supplementary Figure 1. Transmission electron micrographs showing similar core sizes for KID-FtNs (left), KIX-FtNs (middle) and horse spleen ferritin (HSF, right). Scale bar 100 nm. Arrowheads identify several particles in the FtN samples, where individual molecules are more sparsely distributed than in the HSF sample.

Supplementary Figure 2. Coomassie stained SDS-PAGE gel showing the composition of FtNs purified via co-expressed 6His-LF. Transfections included (by DNA amounts) 10% each of HF and LF, 20% 6His-LF and 60% of either KID-LF or KIX-LF. Wild type Ft subunits appear on the gel around 20kDa. 6His-LF is the next band of higher molecular weight. KID-LF and KIX-LF appear between 25kDa and 37kDa.

Supplementary Figure 1

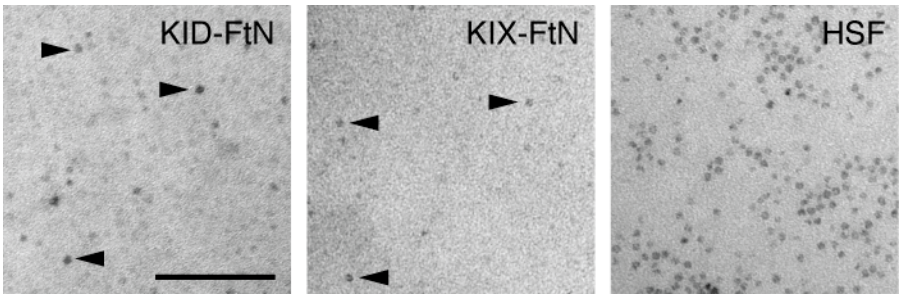

Supplementary Figure 2